

Beyond Anti-Forgetting: Multimodal Continual Instruction Tuning with Positive Forward Transfer

Junhao Zheng, Qianli Ma*, Zhen Liu, Binquan Wu, Huawen Feng
 School of Computer Science and Engineering,
 South China University of Technology, Guangzhou, China
 junhaozheng47@outlook.com, qianlima@scut.edu.cn*

Abstract

Multimodal Continual Instruction Tuning (MCIT) enables Multimodal Large Language Models (MLLMs) to meet continuously emerging requirements without expensive retraining. MCIT faces two major obstacles: catastrophic forgetting (where old knowledge is forgotten) and negative forward transfer (where the performance of future tasks is degraded). Although existing methods have greatly alleviated catastrophic forgetting, they still suffer from negative forward transfer. By performing singular value decomposition (SVD) on input embeddings, we discover a large discrepancy in different input embeddings. The discrepancy results in the model learning irrelevant information for old and pre-trained tasks, which leads to catastrophic forgetting and negative forward transfer. To address these issues, we propose Fwd-Prompt, a prompt-based method projecting prompt gradient to the residual space to minimize the interference between tasks and to the pre-trained subspace for reusing pre-trained knowledge. Our experiments demonstrate that Fwd-Prompt achieves state-of-the-art performance while updating fewer parameters and requiring no old samples. Our research sheds light on the potential of continuously adapting MLLMs to new tasks under the instruction tuning paradigm and encourages future studies to explore MCIT. The code will soon be publicly available.

1 Introduction

Recently, instruction tuning has shown effectiveness in bridging the gap between diverse vision-language tasks and creating general-purpose Multimodal Large Language Models (MLLMs) with broad capabilities [Dai *et al.*, 2023; Liu *et al.*, 2023]. In real-world applications, MLLMs are always expected to learn new vision-language tasks to support new functionalities. However, existing MLLMs are static and can not meet continuously emerging new requirements. To avoid the huge cost of retraining MLLMs, we can formulate this

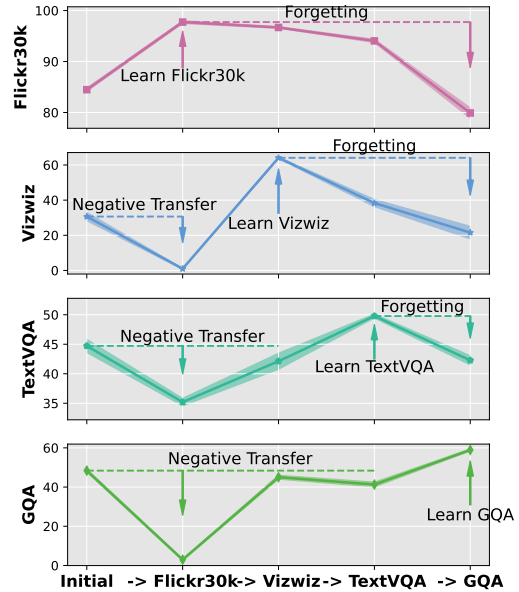


Figure 1: Catastrophic forgetting and negative forward transfer in multimodal continual instruction-tuning. InstructBLIP [Dai *et al.*, 2023] is sequential instruction-tuned on Flickr30k, VizWiz, TextVQA and GQA.

scenario into the paradigm of Multimodal Continual Instruction Tuning (MCIT). In MCIT, we aim to instruction-tune MLLMs for new multimodal tasks incrementally while maintaining superior performance on learned tasks. For example, we start from InstructBILP [Dai *et al.*, 2023], an MLLM instruction-tuned on 13 datasets. Then, we instruction-tune InstructBILP incrementally on Flickr30k [Young *et al.*, 2014], VizWiz [Gurari *et al.*, 2018], TextVQA [Singh *et al.*, 2019], and GQA [Hudson and Manning, 2019]. At last, we expect the final model to perform well on both 4 downstream and 13 pre-trained tasks. Therefore, MCIT is an ideal scenario that equips MLLMs with new skills incrementally without retraining on all datasets.

However, MCIT is particularly challenging. Unlike typical continual learning scenarios, the tasks in MCIT are diverse in terms of input and output format. For example, in Flickr30k, the model outputs a detailed description given an

*.*Corresponding author

image. In GQA, the model outputs a short answer given an image and a question. In TextVQA, the model outputs a short answer given an image, a question, and OCR (Optical Character Recognition) tokens. Therefore, MLLMs are required to generate various responses according to the task instruction.

In this case, MCIT faces two crucial challenges: **catastrophic forgetting** and **negative forward transfer**. By catastrophic forgetting, we mean models forget old knowledge when learning new tasks. For instance, in Fig.1, the performance of Flickr30k (the topmost subfigure) drops significantly when the model is instruction-tuned on new tasks. By negative forward transfer, we mean that the performance of unseen tasks is degraded when learning new tasks. For instance, after instruction-tuning InstructBLIP on Flickr30K, the zero-shot performance on the unseen tasks (i.e., VizWiz, TextVQA, and GQA) is negatively impacted. Addressing negative forward transfer is important because it hinders models from adapting to future tasks. Specifically, the performance of GQA drops from 59.19 to 58.92 after sequential training on Flickr30k, VizWiz and TextVQA compared to direct training on GQA. More results of negative forward transfer can be found in the experiment and the Appendix.

Before introducing our methods, let’s take a closer look at the catastrophic forgetting and negative forward transfer. To achieve anti-forgetting, the old knowledge should be preserved as much as possible. However, in MCIT, not all old knowledge is beneficial for new tasks. For instance, OCR-VQA [Mishra *et al.*, 2019] requires models to recognize the text in images locally while Flickr30k requires to understand the image globally. As shown empirically by He [2023], regularizing old models leads to poor performance on new tasks. In other words, only mitigating catastrophic forgetting may lead to negative forward transfer. Therefore, to avoid both issues, we need to identify what to preserve and update for each task.

We perform SVD [Golub and Reinsch, 1971] on input embeddings to gain more insight. We discover a large **discrepancy** between input embeddings from different tasks. More importantly, the rank of input embeddings decreases when directly instruction-tuning MLLMs on each new task. However, it increases under the continual learning paradigm. This phenomenon indicates that the discrepancy results in models extracting irrelevant input information for old tasks when adapting to new tasks, which leads to catastrophic forgetting. Moreover, the negative forward transfer happens because adapting to the current task results in the model extracting irrelevant information for unseen tasks.

Motivated by these observations, we propose Fwd-Prompt, which achieves anti-forgetting and positive forward transfer. Specifically, Fwd-Prompt proposes selecting prompts according to visual and textual features. On the one hand, Fwd-Prompt achieves anti-forgetting by **allocating different subspaces for each task** and projecting prompt gradient to the residual space. On the other hand, Fwd-Prompt achieves positive forward transfer by **reusing pre-trained knowledge** and projecting prompt gradient to the pre-trained space. Finally, the experiment indicates that Fwd-Prompt achieve state-of-the-art (SOTA) performance on MCIT. In summary, our contribution is three folds:

- We identify that the key challenge of MCIT is to achieve both anti-forgetting and positive forward transfer.
- We analyze the space of input embeddings and reveal that the discrepancy in input embeddings leads to catastrophic forgetting and negative forward transfer.
- To address the two issues, we propose Fwd-Prompt for MCIT, which outperforms SOTA methods by a large margin while requiring less trainable parameters and no rehearsal data.

2 Related Work

2.1 Multimodal Large Language Models

The remarkable capabilities of Multimodal Large Language Models (MLLMs) [OpenAI, 2023] have captured widespread attention within the artificial intelligence community, showcasing their proficiency in comprehending, reasoning, and generating human language. Despite the considerable progress achieved, these methods face challenges when confronted with more complex multimodal information [Mishra *et al.*, 2019; Sidorov *et al.*, 2020; Hudson and Manning, 2019]. Instruction tuning originated from natural language processing and has become a popular strategy for aligning MLLMs with human intent [Touvron *et al.*, 2023; Chiang *et al.*, 2023]. Dai [2023] argue that instruction-tuned MLLMs generalize to unseen tasks better than multitask learning without instructions. They further instruction-tune BLIP2 on 13 high-quality vision-language datasets and proposed InstructBLIP. Motivated by InstructBLIP, recent studies [Panagopoulou *et al.*, 2023; Gong *et al.*, 2023; Wu *et al.*, 2023] further extend instruction-tuning to video, audio, and point cloud modalities. In this study, we focus on vision-language tasks because of their popularity.

2.2 Continual Learning

Although a vast amount of continual learning methods have been proposed in both computer vision and natural language processing, most of them are not applied to MCIT because they are either inapplicable to multimodal tasks [Sun *et al.*, 2019] or computationally expensive for MLLMs [Buzzega *et al.*, 2020]. Recently, prompt-based methods [Wang *et al.*, 2022b; Smith *et al.*, 2023; Wang *et al.*, 2022a] have achieved superior performance on continual image classification. These methods harness the power of pre-trained knowledge by freezing pre-trained models and learning only soft prompts for continual learning. Inspired by their success in mitigating forgetting, we further employ the idea of gradient projection [Saha *et al.*, 2021] to encourage positive forward transfer.

2.3 MLLMs for Continual Learning

Continual learning with MLLMs is an emerging research field. Existing research can be divided into two categories: continual learning of visual question answering (VQA) and continual vision-language pretraining. (1) continual learning of visual question answering (VQA): Srinivasan [2022] proposes CLiMB, a continual learning benchmark for vision-language, vision-only and language-only

classification tasks. CL-CrossVQA [Zhang *et al.*, 2022] and VQACL [Zhang *et al.*, 2023] are two benchmarks for cross-domain VQA and VQA with skill-concept compositions, respectively. Qian [2023] designs special strategies for interactions between modalities. (2) continual vision-language pre-training: These methods [Ni *et al.*, 2023; Zheng *et al.*, 2023; Zhu *et al.*, 2023] aim at aligning vision and language features. Unlike continual VQA, the models are trained on image-text pairs and typically evaluated on retrieval or zero-shot classification tasks.

Unlike the studies above, we explore the continual learning scenario of instruction tuning. There are two key differences between MCIT and the aforementioned continual scenario. (1) The MLLM outputs natural language directly and requires no additional classifiers. (2) MCIT allows MLLMs to learn diverse tasks beyond VQA, including image captioning, image captioning with OCR tokens, and VQA with OCR tokens. This study evaluates Fwd-Prompt on the MCIT benchmark proposed in [He *et al.*, 2023].

3 Preliminaries

3.1 Prompt-Based Continual Learning

Prompt-based continual learning is first proposed by Wang [2022b]. Typically, there is a set of key-value pairs called prompt pool $\mathcal{P} = \{k_j, p_j\}_j^M$, where M is the number of total key-value pairs, $k_j, p_j \in \mathbb{R}^d$ represent the j -th key and value, respectively. For an input image x_i , its query feature is computed as $q_i = f^{(img)}(x_i)$, where $f^{(img)}(\cdot)$ is usually a pre-trained and frozen Vision Transformer (ViT). Then, we select the top- n_p prompts according to the cosine similarity between q_i and all keys in the prompt pool. Finally, we concatenate the selected prompts to the input embeddings of x_i and feed them into the backbone model such as ViT.

3.2 Singular Value Decomposition

Singular Value Decomposition (SVD) [Golub and Reinsch, 1971] is useful in linear algebra. Typically, the singular value decomposition of an matrix $A \in \mathbb{R}^{M \times N}$ is $A = U\Sigma V^T$, where $U \in \mathbb{R}^{M \times M}$ and $V \in \mathbb{R}^{N \times N}$ are two orthogonal matrices, and $\Sigma \in \mathbb{R}^{M \times N}$ is a rectangular diagonal matrix. The columns of U and V form two sets of orthonormal bases called left-singular vectors $\{u_1, u_2, \dots, u_M\}$ and right-singular vectors $\{v_1, v_2, \dots, v_N\}$. The main diagonal of Σ is the singular values $\sigma_1, \sigma_2, \dots, \sigma_r$, where $r < \min\{M, N\}$ is the rank of A and the singular values are sorted in a descending order.

We can regard A as a transformation from \mathbb{R}^N to \mathbb{R}^M . Then, v_1 is the unit vector that is maximally stretched by A , i.e., $\arg \max_{x: \|x\|_2=1} \|Ax\|_2 = v_1$. We provide a brief proof as follows. First, we convert the objective as follows: $\arg \max_{x: \|x\|_2=1} \|Ax\|_2 = \arg \max_{x: \|x\|_2=1} \|Ax\|_2^2 = \arg \max_{x: \|x\|_2=1} x^T A^T A x$. Since the eigenvalue expression of $A^T A$ is $(A^T A)x = \lambda x$, we have $x^T A^T A x = \lambda$. Then, the objective is converted to choose x as the eigenvector with the largest eigenvalue. Because $A^T A = V\Sigma^2 V^T$ and V is given by the eigendecomposition of $A^T A$, v_1 is exactly the unit vector that maximizes the objective $\|Ax\|_2$. Similarly,

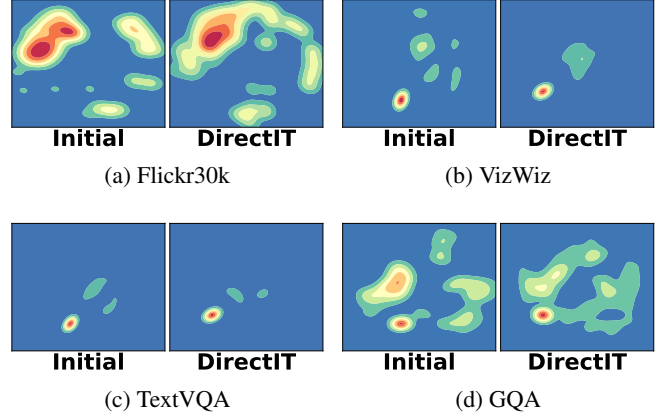


Figure 2: The contour of the distribution of input embeddings from four different tasks. “Initial” and “DirectIT” represent the input embeddings of InstructBLIP before and after instruction tuning on each task, respectively.

we can prove that v_N is the unit vector minimally stretched by A .

Furthermore, we can divide V into two orthogonal subspace $V_{core} = [v_1, v_2, \dots, v_K]$ and $V_{res} = [v_{K+1}, v_{K+2}, \dots, v_N]$ by selecting the first K and the remaining eigenvectors, denoted as the **core space** and the **residual space** respectively. Since $VV^T = I$ and I represents the identity matrix, we have $V_{core}V_{core}^T + V_{res}V_{res}^T = I$. For an arbitrary vector x , we can decompose it into the core and residual space as $x = x_{core} + x_{res}$, where $x_{core} = V_{core}V_{core}^T x$ and $x_{res} = V_{res}V_{res}^T x$. Then, the output vector of x_{core} (i.e., Ax_{core}) has a large norm, while the output vector of x_{res} has a small norm. In this way, we can control the impact of x on the output vector by mapping it into different subspaces before multiplying with A .

4 Methodology

In Sec.4.1, we qualitatively and quantitatively analyze the input embedding space in continual learning to gain insights for forgetting and forward transfer. We describe Fwd-Prompt in Sec.4.2,4.3, and 4.4.

4.1 A Closer Look at the Forgetting and Negative Forward Transfer

MCIT is challenging since there is a considerable input and output format discrepancy across tasks. To understand how this affects model performance, we visualize the input embeddings of each task before (Initial) and after (DirectIT) instruction-tuning InstructBLIP on each task. InstructBLIP only trains Q-Former to align the visual and textual features while keeping the ViT and LLM frozen. Here, input embeddings refer to the visual and textual embeddings extracted by Q-Former for feeding into the LLM.

Fig.2 shows that the distribution of input embeddings has a large discrepancy across tasks. Specifically, we find that Flickr30k has a broader distribution than the other three VQA-based tasks, suggesting that image captioning requires

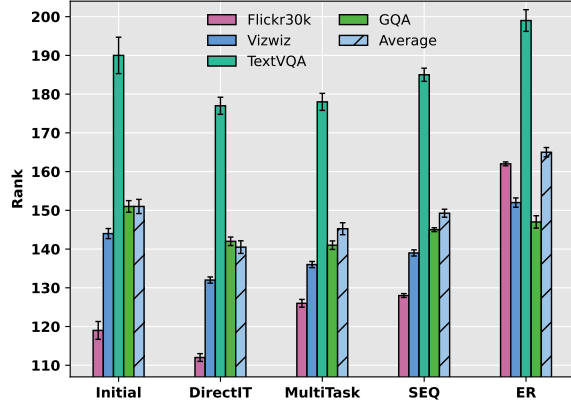


Figure 3: The rank of input embeddings in five scenarios. “Initial”: load InstructBLIP without training; “DirectIT”: train InstructBLIP on the four datasets respectively; “MultiTask”: train InstructBLIP on all four datasets jointly; “SEQ”: train InstructBLIP on the four datasets sequentially; “ER”: store 1 % of old instances and train InstructBLIP sequentially using the experience replay strategy. “Initial” is a starting point of MCIT. “DirectIT” and “MultiTask” are both the upper bound of MCIT and “SEQ” is the lower bound. “ER” is a popular technique for alleviating forgetting.

detailed information from the input image. It explains that the performance degradation of VQA-based tasks when learning Flickr30k (Fig.1) caused by the differences of the information required for each task. Fig.2 also shows that the distribution of “Initial” and “DirectIT” is similar. It indicates that the required information is relatively stable during instruction-tuning.

To quantitatively analyze the changes of input embeddings during continual learning, we estimate the rank of input embeddings with threshold $\epsilon = 0.99$. Fig.3 shows that “DirectIT” and “MultiTask” have a lower rank than “Initial”. It indicates that all tasks can be jointly learned without introducing additional input information. However, under continual learning scenarios (“SEQ” and “ER”), the rank of old tasks (Flickr30k, VizWiz, and TextVQA) increases significantly. It indicates that the model learns to extract irrelevant input information for old tasks when adapting to new tasks, which leads to catastrophic forgetting. From this perspective, the negative forward transfer happens because adapting to the current task results in the model extracting irrelevant information for unseen tasks.

4.2 Prompt-Based Continual Learning for MCIT

We provide an overview of Fwd-Prompt in Fig.4a. This subsection describes how to design a prompt pool for multimodal tasks.

Intuitively, it is easier for the model to output the correct answer if task-specific descriptions such as “This task requires reading the text on books” or instance-specific descriptions such as “This photo was taken at a fast food restaurant” are provided. Therefore, we follow L2P [Wang *et al.*, 2022b] and design a prompt pool where soft prompts are selected dynamically according to each instance. In MCIT, the output is determined by both the input image and instruction. For

instance, given the same input image in Fig.4a, the expected output would be “Cola” if the instruction is changed to “What is the name of the drink on the upper left corner?”. Therefore, each prompt should be determined by both image and instruction. To achieve this, we design two keys for each prompt and the prompt pool is defined as $\mathcal{P} = \{k_j^{(img)}, k_j^{(text)}, p_j\}_j^M$, where M is the number of total key-value pairs, $p_j \in \mathbb{R}^d$ represent the j -th value, $k_j^{(img)} \in \mathbb{R}^{d_i}$ and $k_j^{(text)} \in \mathbb{R}^{d_t}$ represent the key for image and instruction respectively. d , d_i and d_t are the dimensions of input embeddings, visual and textual features, respectively. For the i -th instance containing an image $x_i^{(img)}$ and instruction $x_i^{(text)}$, its similarity with the j -th prompt is calculated as

$$\phi_{i,j} = \phi(q_i^{(img)}, k_j^{(img)}) + \phi(q_i^{(text)}, k_j^{(text)}), \quad (1)$$

where $q_i^{(img)}$ is the query of $x_i^{(img)}$ and is obtained by averaging the features from a frozen vision encoder such as ViT-g/14 [Fang *et al.*, 2023] used in InstructBLIP. Similarly, $q_i^{(text)}$ is the query of $x_i^{(text)}$ and is obtained by averaging the input embeddings of LLM such as Flan-T5 [Chung *et al.*, 2022] used in InstructBLIP. $\phi(q_i^{(img)}, k_j^{(img)})$ is computed as the cosine similarity between $q_i^{(img)}$ and $k_j^{(img)}$ normalized over all keys in the prompt pool with softmax function. And $\phi(q_i^{(text)}, k_j^{(text)})$ is computed in a similar way.

4.3 Anti-Forgetting for Prompt Tuning

This section describes how to achieve anti-forgetting when utilizing prompt tuning for continual learning.

To achieve the goal of anti-forgetting, we expect the model to output the same response given the same image and instruction when soft prompts are updated. Formally, we have

$$f_{LLM}([p_{t+1}^T; e_t^{(img)}; e_t^{(text)}]) = f_{LLM}([p_t^T; e_t^{(img)}; e_t^{(text)}]), \quad (2)$$

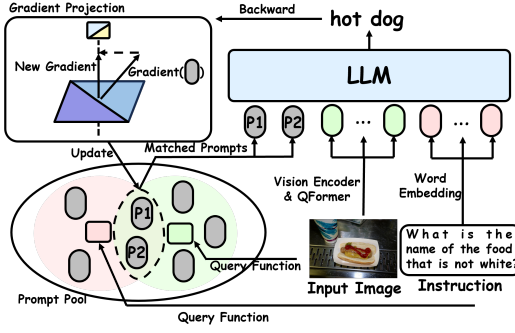
where f_{LLM} represents the large language model, and it is frozen during continual learning. $p_{t+1}, p_t \in \mathbb{R}^d$ are the prompts before and after the update of task t . We consider only one prompt for demonstration purposes. $e_t^{(img)} \in \mathbb{R}^{n_i \times d}$, $e_t^{(text)} \in \mathbb{R}^{n_t \times d}$ represent the n_i, n_t input embedding tokens corresponding to the input image and instruction from task t . $[p_{t+1}^T; e_t^{(img)}; e_t^{(text)}]$ represents that the prompt is concatenated with the input along the sequence dimension. To achieve Eq.2, the prompt and input embeddings should satisfy the following relationship:

$$\begin{cases} p_{t+1}^T p_{t+1} = p_t^T p_t & (3) \end{cases}$$

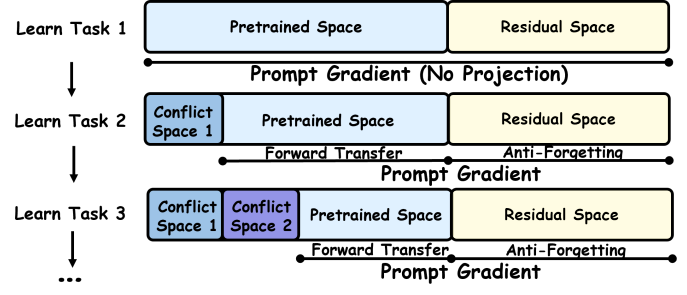
$$\begin{cases} e_t^{(img)} \Delta p = O & (4) \end{cases}$$

$$\begin{cases} e_t^{(text)} \Delta p = O. & (5) \end{cases}$$

$\Delta p = p_{t+1} - p_t$ can be regarded as the gradient of the prompt. We provide the detailed derivation in the Appendix. Eq.3 indicates that the updated prompt should have the same L2 norm. In practice, the learned prompts have relatively close L2 norms, and thus, the first constraint is ignored in our implementation. The latter two constraints in Eq.4 and 5 indicate that the prompt gradient should be orthogonal to the



(a) Overview of Fwd-Prompt



(b) Gradient Projection in Fwd-Prompt

Figure 4: (a) An overview of Fwd-Prompt. The details of prompt pool and gradient projection are in Sec.4.2 and 4.4. (b) An illustration of the gradient projection in Fwd-Prompt.

input embeddings of both image and instruction. To satisfy these constraints, we perform SVD on the concatenated input embeddings $e_t^{(joint)} = [e_t^{(img)}; e_t^{(text)}] \in \mathbb{R}^{(n_i+n_t) \times d}$ and obtain d right singular vectors $\{v_1, v_2, \dots, v_d\}$. Then, select the first K right singular vectors to form the **core space** of task t that satisfy $\|e_t^{(joint)}\| \geq \epsilon \|e_t^{(joint)}\|$, where $e_t^{(joint)}$ is the **K-rank approximation** of $e_t^{(joint)}$, $\|\cdot\|$ represent the Frobenius norm, and $\epsilon = 0.99$. The remaining $d - K$ right singular vectors form the **residual space** of task t . After obtaining the prompt gradient Δp , we project Δp to the residual space as follows: $\Delta p' = V_{res} V_{res}^T \Delta p$, where $V_{res} = [v_{k+1}, v_{k+2}, \dots, v_d] \in \mathbb{R}^{d \times (d-K)}$. By mapping the prompt gradient into the residual subspace, the forgetting of the knowledge of task t is minimized.

4.4 Anti-Forgetting and Positive Forward Transfer with Gradient Projection

In this subsection, we will extend the idea in Sec.4.3 and achieve positive forward transfer beyond anti-forgetting. The fundamental intuition is to reuse the pre-trained knowledge during continual learning to avoid extracting irrelevant input information for unseen tasks as described in Sec.4.1. An illustration for gradient projection in Fwd-Prompt is provided in Fig.4b.

Specifically, we regard the pre-trained tasks before continual learning as task 0 and identify its **pre-trained space** and **residual space** using K -rank approximation as described in Sec.4.3. We denote the pre-trained space as $V_{pre} \in \mathbb{R}^{d \times K_0}$ and the residual space as $V_{res} \in \mathbb{R}^{d \times (d-K_0)}$.

When adapting to task 1, we train the prompt pool without gradient projection. After finishing the training on task 1, we perform SVD on the input embeddings from task 1 and obtain the core space of task 1 (denoted as V_{core}^1) by K -rank approximation. Then, we record the indexes of directions in the pre-trained space that conflicts with the core space of task 1. Formally, the conflicting index set \mathcal{I}^1 for task 1 is calculated as follows:

$$\mathcal{I}^1 = \{i | \exists j, |\cosine(V_{pre}[:, i], V_{core}^1[:, j])| > \theta\}, \quad (6)$$

where $V_{pre}[:, i], V_{core}^1[:, j]$ represent the i -th and j -th column

vectors in V_{pre} and V_{core}^1 respectively. θ is the threshold for determining if two directions are overlapping. $\cosine(\cdot, \cdot)$ computes the cosine similarity between two vectors. And then, we define the **conflicting space of task 1** as follows:

$$V_{con}^1 = \{V_{pre}[:, i]\}_{i \in \mathcal{I}^1}. \quad (7)$$

When adapting to task 2, the prompt gradient is projected to the orthogonal direction of V_{con}^1 to avoid forgetting the knowledge in task 1:

$$\Delta p' = (I - V_{con}^1 V_{con}^{1T}) \Delta p, \quad (8)$$

After finishing training on task 2, we find the conflicting index set \mathcal{I}^2 for task 2 in a similar way. Similarly, when adapting to task 3, the prompt gradient is computed as follows:

$$\Delta p' = (I - V_{con}^{1,2} V_{con}^{1,2T}) \Delta p. \quad (9)$$

$$V_{con}^{1,2} = \{V_{pre}[:, i]\}_{i \in \mathcal{I}^1 \cup \mathcal{I}^2}. \quad (10)$$

In summary, Fwd-Prompt avoids interference between new tasks by allocating different conflicting spaces and projecting gradients to the residual space, thus achieving anti-forgetting. Furthermore, Fwd-Prompt reuses pre-trained knowledge by updating prompts in the pre-trained space, which contains the core space of unseen tasks, thus enhancing positive forward transfer.

5 Experiment

5.1 Experimental Settings

Datasets. We evaluate Fwd-Prompt on the benchmark proposed by He [2023]. We consider two MLLMs, InstructBLIP (FlanT5XL) model and BLIP2 (FlanT5XL) [Li et al., 2023b] for continual learning. The experimental result of BLIP2 is in the Appendix. When using InstructBLIP as the starting point, the task order is Flickr30K, VizWiz, TextVQA, and GQA. Besides, we expect InstructBLIP to preserve the pre-trained knowledge obtained during joint instruction-tuning before continual learning. Therefore, we evaluate InstructBLIP on six pre-trained tasks: Caption COCO [Chen et al., 2015], TextCaps [Sidorov et al., 2020], VQAv2 [Goyal et al., 2017], OKVQA [Marino et al., 2019], A-OKVQA [Schwenk et al., 2022], OCR-VQA [Mishra et al., 2019].

Table 1: Comparison with SOTA methods for MCIT. The average accuracy after learning the final task is reported, i.e. \mathcal{A}_4 . The average accuracy of each incremental step and other metrics are reported in Fig.5. The backbone model is InstructBLIP. “ER” and “EProj” require storing 1% of old samples for rehearsal.

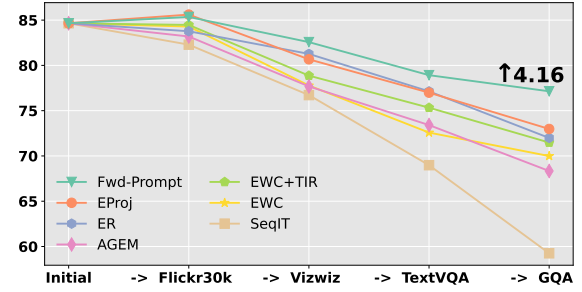
Datasets	Non-CL Baselines		CL Baselines						
	Initial	DirectIT	SeqIT	EWC	EWC_TIR	AGEM	ER	EProj	Fwd-Prompt (Ours)
Caption Coco	140.81	140.81	115.85	128.27	130.77	121.89	<u>135.00</u>	134.99	137.58
TextCaps	127.08	127.08	86.02	120.15	121.71	114.72	122.75	126.75	<u>125.50</u>
VQAv2	73.47	73.47	61.08	71.54	<u>71.96</u>	68.31	67.06	68.03	72.98
OKVQA	48.84	48.84	30.55	44.77	<u>45.44</u>	40.76	37.49	41.12	48.68
AOKVQA	55.31	55.31	38.52	53.16	<u>53.51</u>	44.88	45.68	51.85	53.97
OCR-VQA	62.37	62.37	57.84	60.28	<u>62.30</u>	60.37	61.38	62.36	61.78
Flickr30k	84.87	97.74	79.91	92.10	<u>94.70</u>	90.68	95.98	97.99	97.53
VizWiz	30.65	64.58	21.54	31.14	33.53	37.83	<u>46.36</u>	45.05	62.79
TextVQA	44.72	51.10	42.28	48.09	<u>49.38</u>	47.25	49.19	47.58	50.08
GQA	48.38	59.19	58.92	50.26	51.45	56.31	<u>59.02</u>	54.06	60.52
Average	71.65	78.05	59.25	69.98	71.48	68.30	71.99	<u>72.97</u>	77.14
Improvement	/	/	0.00	+10.73	+12.22	+9.05	+12.74	<u>+13.73</u>	+17.89
Trainable Params	/	/	187M	187M	187M	187M	187M	189M	48.5M
Use Old Samples	/	/	✗	✗	✗	✗	✓	✓	✗

Metric. We adopt top-1 accuracy as the metric for VQA-based tasks and CIDEr for image-captioning tasks. We report three metrics for continual learning, including average accuracy (\mathcal{A}_t , higher is better), forgetting (FGT_t , lower is better), and forward transfer (FWD_t , higher is better) after learning task t . Specifically, $\mathcal{A}_t = \frac{1}{t} \sum_{i=1}^t a_{t,i}$, where $a_{t,i}$ is the performance score of task i after learning task t . The forgetting is computed as the average performance degradation of all learned tasks: $FGT_t = \frac{1}{t-1} \sum_{i=1}^{t-1} [\max_{j < t} (\{a_{j,i}\}_j) - a_{t,i}]$. The forward transfer is computed as the difference between continual learning and direct instruction-tuning on task t : $FWD_t = a_{t,t} - a_t$. When $FWD_t > 0$, it implies positive forward transfer for learning task t . When $FWD_t < 0$, it implies negative forward transfer for learning task t .

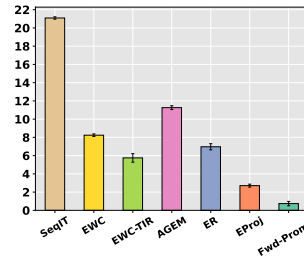
Hyper-Parameters. We set the number of key-values pairs $M = 20$, the threshold for k -rank approximation $\epsilon = 0.99$, the threshold for finding matching directions $\theta = 0.5$, the number of selected prompts for input $n_p = 5$.

Baselines. We consider 6 baselines for continual learning, including sequential instruction-tuning (SeqIT), EWC [Kirkpatrick *et al.*, 2017], EWC_TIR [He *et al.*, 2023], AGEM [Chaudhry *et al.*, 2019], experience replay (ER), EProj [He *et al.*, 2023]. EProj is the current state-of-the-art (SOTA) method for MCIT. Besides, we compare two **non-continual learning** baselines: InstructBLIP before continual learning (Initial) and instruction-tuned on each new task, respectively (DirectIT). SeqIT and DirectIT are the lower and upper bounds for continual learning.

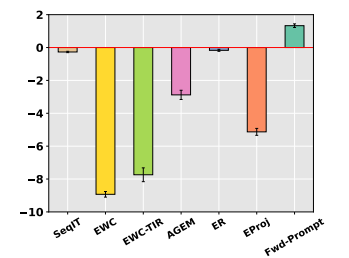
Implementation Details. We use the implementation of InstructBLIP, and BLIP2 provided in the LAVIS library [Li *et al.*, 2023a]. We train GQA for 1 epoch and other tasks for 5 epochs with an initial learning rate of $1e-5$. The batch size is set as 32. In EProj, the projection layer is expanded for each new task and task keys are learned for selecting task ID during inference. For a fair comparison, Fwd-Prompt follows EProj and additionally learns new projection layers and task keys. Due to the flexibility of prompt tuning, Fwd-Prompt only trains the top 3 layers in Q-Former rather than the entire



(a) Average Accuracy $\mathcal{A}_t \uparrow$



(b) Forgetting $FGT_4 \downarrow$



(c) Forward Transfer $FWD_4 \uparrow$

Figure 5: Comparison with SOTA methods in terms of average accuracy, forgetting and forward transfer.

Q-Former as it does in InstructBLIP. More implementation details are provided in the Appendix.

5.2 Result and Analysis

Comparison with SOTA Methods. Table 1 and Fig.5 demonstrate the SOTA performance of Fwd-Prompt. Despite storing no old samples and training fewer parameters, Fwd-Prompt outperforms the previous SOTA method by 4.16%. It is worth noting that regularization-based methods such as EWC, EWC_TIR, and AGEM suffer from negative forward transfer greatly, while replay-based methods suffer from either catastrophic forgetting or negative forward transfer.

Table 2: The ablation study and hyper-parameter analysis for Fwd-Prompt.

	Method	\mathcal{A}_4	Δ
Ours	Fwd-Prompt	77.14	0.00
	w/o Prompt Pool	63.59	-13.55
Ablation	w/o Gradient Projection	74.82	-2.32
	Separated Prompt Pools	74.71	-2.43
Variation	More Prompt Tokens $n_p = 10$	76.85	-0.29
	Larger Prompt Pool $M = 40$	77.31	+0.17
	Both $M = 40, n_p = 10$	76.89	-0.25
	Threshold $\epsilon = 0.90$	75.93	-1.21
	Threshold $\epsilon = 0.95$	76.50	-0.64

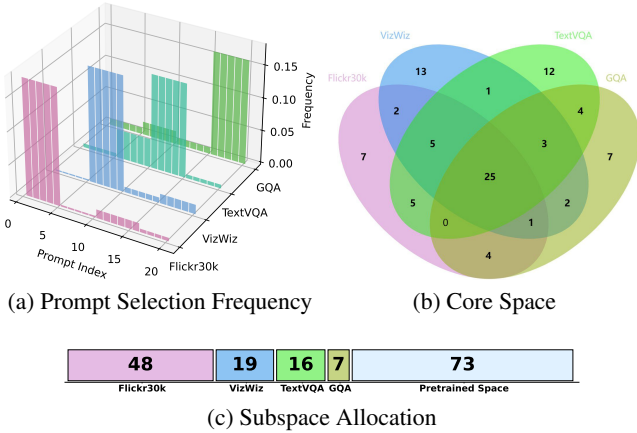


Figure 6: The forward transfer in Fwd-Prompt. (a) The histogram of prompt selection frequency. (b) The Venn diagram of the column vectors in the core space. (c) The subspace allocation in Fwd-Prompt.

Fwd-Prompt harnesses the power of LLM with prompt tuning and enhances positive forward transfer with gradient projection.

Ablation Study and Hyper-Parameter Analysis. We consider two ablated versions and six variations for Fwd-Prompt. Table 2 shows that both the prompt pool and the gradient projection are the keys to the success of Fwd-Prompt. “Separated Prompt Pools” represents training two prompt pools separately for vision and instruction input. The results show that “Separated Prompt Pools” leads to much worse performance, suggesting selecting prompts with information from both modalities is crucial. Besides, the results show that a larger prompt pool leads to better performance while prepending more prompt tokens does not. We speculate the reason is that more prompt tokens are harder to train.

Visualization of Forward Transfer. Fig.6 visualizes the forward transfer in Fwd-Prompt. As shown in Fig.6a, each task corresponds to a non-overlapping set of prompts, and the interaction across tasks is weak. This is because the gap between tasks is large, and the model learns task-specific information during training. Our finding is consistent with L2P [Wang *et al.*, 2022b]. Fig.6b shows a considerable overlap

[Input Image]	[Input Instruction]	[Model Response]	
	A short image description:	[Fwd-Prompt]	A white and red bus drives on a busy on a four lane road with other vehicles.
		[EProj]	A white bus is driving on a highway leading to a turn
	Question: I was wondering how ominous the sky is looking here at the northwest. Short answer:	[Fwd-Prompt]	dark cloudy
		[EProj]	unanswerable

Figure 7: Comparison between Fwd-Prompt and EProj after learning the final task in MCIT. The upper and lower rows are instances from the dev set of a pre-trained task, Caption COCO, and a new task in continual learning, VizWiz.

Table 3: Comparison with SOTA methods in training time of continual learning.

Method	Run Time (min)	Ratio	Method	Run Time (min)	Ratio
SeqIT	502	$\times 1.0$	EWC	745	$\times 1.5$
EWC.TIR	768	$\times 1.5$	A-GEM	1047	$\times 2.1$
ER	945	$\times 1.9$	EProj	972	$\times 1.9$
Fwd-Prompt	660	$\times 1.3$			

in the core space of different tasks. Fwd-Prompt avoids conflict between tasks by allocating different conflicting spaces to different tasks. Fig.6c visualizes the subspace allocation in Fwd-Prompt. For example, when the model learns the first task, Flickr30k, the conflicting space 1 is all 48 directions in the core space of Flickr30k. When the model learns the second task, VizWiz, the conflicting space 2 is the direction in the core space of VizWiz minus those of Flickr30k. In this way, Fwd-Prompt avoids the interference between new tasks and thus achieves anti-forgetting. Furthermore, Fwd-Prompt enhances positive forward transfer by updating prompts in the pre-trained space, which contains the core space of unseen tasks.

Case Study. As shown in Fig.7, the responses of Fwd-Prompt in two instances are more visually grounded than EProj. It indicates that Fwd-Prompt better preserves knowledge gained before and after continual learning.

Run Time Analysis. The comparison of training time is shown in Table 3. Although Fwd-Prompt requires an additional 30% training time than SeqIT, it requires less training time than other continual learning baselines, demonstrating its superior practicability in real-world scenarios.

6 Conclusion and Limitation

In this paper, we analyze the input embeddings and reveal that the conflict in input embeddings leads to forgetting and negative forward transfer. To this end, we present Fwd-Prompt, a novel approach to addressing the critical challenges of catastrophic forgetting and negative forward transfer in MCIT. The experimental results show that Fwd-Prompt outperforms SOTA methods significantly while requiring less training time, trainable parameters and no old samples.

There are two limitations of this research: (1) This research

does not fully explain the overlapping knowledge between tasks; (2) The number of tasks in MCIT is limited.

References

- [Boix-Adsera *et al.*, 2023] Enric Boix-Adsera, Etai Littwin, Emmanuel Abbe, Samy Bengio, and Joshua Susskind. Transformers learn through gradual rank increase. *arXiv preprint arXiv:2306.07042*, 2023.
- [Buzzega *et al.*, 2020] Pietro Buzzega, Matteo Boschini, Angelo Porrello, Davide Abati, and Simone Calderara. Dark experience for general continual learning: a strong, simple baseline. *Advances in neural information processing systems*, 33:15920–15930, 2020.
- [Chaudhry *et al.*, 2019] Arslan Chaudhry, Marc’Aurelio Ranzato, Marcus Rohrbach, and Mohamed Elhoseiny. Efficient lifelong learning with a-gem. In *International Conference on Learning Representations*, 2019.
- [Chen *et al.*, 2015] Xinlei Chen, Hao Fang, Tsung-Yi Lin, Ramakrishna Vedantam, Saurabh Gupta, Piotr Dollár, and C Lawrence Zitnick. Microsoft coco captions: Data collection and evaluation server. *arXiv preprint arXiv:1504.00325*, 2015.
- [Chiang *et al.*, 2023] Wei-Lin Chiang, Zhuohan Li, Zi Lin, Ying Sheng, Zhanghao Wu, Hao Zhang, Lianmin Zheng, Siyuan Zhuang, Yonghao Zhuang, Joseph E Gonzalez, et al. Vicuna: An open-source chatbot impressing gpt-4 with 90%* chatgpt quality. See <https://vicuna.lmsys.org> (accessed 14 April 2023), 2023.
- [Chung *et al.*, 2022] Hyung Won Chung, Le Hou, Shayne Longpre, Barret Zoph, Yi Tay, William Fedus, Yunxuan Li, Xuezhi Wang, Mostafa Dehghani, Siddhartha Brahma, et al. Scaling instruction-finetuned language models. *arXiv preprint arXiv:2210.11416*, 2022.
- [Dai *et al.*, 2023] Wenliang Dai, Junnan Li, Dongxu Li, Anthony Meng Huat Tiong, Junqi Zhao, Weisheng Wang, Boyang Li, Pascale Fung, and Steven Hoi. Instructblip: Towards general-purpose vision-language models with instruction tuning, 2023.
- [Fang *et al.*, 2023] Yuxin Fang, Wen Wang, Binhui Xie, Quan Sun, Ledell Wu, Xinggang Wang, Tiejun Huang, Xinlong Wang, and Yue Cao. Eva: Exploring the limits of masked visual representation learning at scale. In *Proceedings of the IEEE/CVF Conference on Computer Vision and Pattern Recognition*, pages 19358–19369, 2023.
- [Golub and Reinsch, 1971] Gene H Golub and Christian Reinsch. Singular value decomposition and least squares solutions. In *Handbook for Automatic Computation: Volume II: Linear Algebra*, pages 134–151. Springer, 1971.
- [Gong *et al.*, 2023] Tao Gong, Chengqi Lyu, Shilong Zhang, Yudong Wang, Miao Zheng, Qian Zhao, Kuikun Liu, Wenwei Zhang, Ping Luo, and Kai Chen. Multimodal-gpt: A vision and language model for dialogue with humans. *arXiv preprint arXiv:2305.04790*, 2023.
- [Goyal *et al.*, 2017] Yash Goyal, Tejas Khot, Douglas Summers-Stay, Dhruv Batra, and Devi Parikh. Making the v in vqa matter: Elevating the role of image understanding in visual question answering. In *Proceedings of the IEEE conference on computer vision and pattern recognition*, pages 6904–6913, 2017.
- [Gurari *et al.*, 2018] Danna Gurari, Qing Li, Abigale J Stangl, Anhong Guo, Chi Lin, Kristen Grauman, Jiebo Luo, and Jeffrey P Bigham. Vizwiz grand challenge: Answering visual questions from blind people. In *Proceedings of the IEEE conference on computer vision and pattern recognition*, pages 3608–3617, 2018.
- [He *et al.*, 2023] Jinghan He, Haiyun Guo, Ming Tang, and Jinqiao Wang. Continual instruction tuning for large multimodal models. *arXiv preprint arXiv:2311.16206*, 2023.
- [Hudson and Manning, 2019] Drew A Hudson and Christopher D Manning. Gqa: A new dataset for real-world visual reasoning and compositional question answering. In *Proceedings of the IEEE/CVF conference on computer vision and pattern recognition*, pages 6700–6709, 2019.
- [Kirkpatrick *et al.*, 2017] James Kirkpatrick, Razvan Pascanu, Neil Rabinowitz, Joel Veness, Guillaume Desjardins, Andrei A Rusu, Kieran Milan, John Quan, Tiago Ramalho, Agnieszka Grabska-Barwinska, et al. Overcoming catastrophic forgetting in neural networks. *Proceedings of the national academy of sciences*, 114(13):3521–3526, 2017.
- [Li *et al.*, 2023a] Dongxu Li, Junnan Li, Hung Le, Guangsen Wang, Silvio Savarese, and Steven CH Hoi. Lavis: A one-stop library for language-vision intelligence. In *Proceedings of the 61st Annual Meeting of the Association for Computational Linguistics (Volume 3: System Demonstrations)*, pages 31–41, 2023.
- [Li *et al.*, 2023b] Junnan Li, Dongxu Li, Silvio Savarese, and Steven Hoi. Blip-2: Bootstrapping language-image pre-training with frozen image encoders and large language models. *arXiv preprint arXiv:2301.12597*, 2023.
- [Liu *et al.*, 2023] Haotian Liu, Chunyuan Li, Qingyang Wu, and Yong Jae Lee. Visual instruction tuning. *arXiv preprint arXiv:2304.08485*, 2023.
- [Marino *et al.*, 2019] Kenneth Marino, Mohammad Rastegari, Ali Farhadi, and Roozbeh Mottaghi. Ok-vqa: A visual question answering benchmark requiring external knowledge. In *Proceedings of the IEEE/cvf conference on computer vision and pattern recognition*, pages 3195–3204, 2019.
- [Mishra *et al.*, 2019] Anand Mishra, Shashank Shekhar, Ajeet Kumar Singh, and Anirban Chakraborty. Ocr-vqa: Visual question answering by reading text in images. In *2019 international conference on document analysis and recognition (ICDAR)*, pages 947–952. IEEE, 2019.
- [Ni *et al.*, 2023] Zixuan Ni, Longhui Wei, Siliang Tang, Yueting Zhuang, and Qi Tian. Continual vision-language representation learning with off-diagonal information. 2023.
- [OpenAI, 2023] OpenAI. Gpt-4 technical report, 2023.

- [Panagopoulou *et al.*, 2023] Artemis Panagopoulou, Le Xue, Ning Yu, Junnan Li, Dongxu Li, Shafiq Joty, Ran Xu, Silvio Savarese, Caiming Xiong, and Juan Carlos Niebles. X-instructblip: A framework for aligning x-modal instruction-aware representations to llms and emergent cross-modal reasoning. *arXiv preprint arXiv:2311.18799*, 2023.
- [Qian *et al.*, 2023] Zi Qian, Xin Wang, Xuguang Duan, Pengda Qin, Yuhong Li, and Wenwu Zhu. Decouple before interact: Multi-modal prompt learning for continual visual question answering. In *Proceedings of the IEEE/CVF International Conference on Computer Vision*, pages 2953–2962, 2023.
- [Saha *et al.*, 2021] Gobinda Saha, Isha Garg, and Kaushik Roy. Gradient projection memory for continual learning. In *International Conference on Learning Representations*, 2021.
- [Schwenk *et al.*, 2022] Dustin Schwenk, Apoorv Khandelwal, Christopher Clark, Kenneth Marino, and Roozbeh Mottaghi. A-okvqa: A benchmark for visual question answering using world knowledge. In *European Conference on Computer Vision*, pages 146–162. Springer, 2022.
- [Sidorov *et al.*, 2020] Oleksii Sidorov, Ronghang Hu, Marcus Rohrbach, and Amanpreet Singh. Textcaps: a dataset for image captioning with reading comprehension. In *Computer Vision—ECCV 2020: 16th European Conference, Glasgow, UK, August 23–28, 2020, Proceedings, Part II 16*, pages 742–758. Springer, 2020.
- [Singh *et al.*, 2019] Amanpreet Singh, Vivek Natarajan, Meet Shah, Yu Jiang, Xinlei Chen, Dhruv Batra, Devi Parikh, and Marcus Rohrbach. Towards vqa models that can read. In *Proceedings of the IEEE/CVF conference on computer vision and pattern recognition*, pages 8317–8326, 2019.
- [Smith *et al.*, 2023] James Seale Smith, Leonid Karlinsky, Vyshnavi Gutta, Paola Cascante-Bonilla, Donghyun Kim, Assaf Arbelle, Rameswar Panda, Rogerio Feris, and Zsolt Kira. Coda-prompt: Continual decomposed attention-based prompting for rehearsal-free continual learning. In *Proceedings of the IEEE/CVF Conference on Computer Vision and Pattern Recognition*, pages 11909–11919, 2023.
- [Srinivasan *et al.*, 2022] Tejas Srinivasan, Ting-Yun Chang, Leticia Pinto Alva, Georgios Chochlakis, Mohammad Rostami, and Jesse Thomason. Climb: A continual learning benchmark for vision-and-language tasks. *Advances in Neural Information Processing Systems*, 35:29440–29453, 2022.
- [Sun *et al.*, 2019] Fan-Keng Sun, Cheng-Hao Ho, and Hung-Yi Lee. Lamol: Language modeling for lifelong language learning. *arXiv preprint arXiv:1909.03329*, 2019.
- [Touvron *et al.*, 2023] Hugo Touvron, Thibaut Lavril, Gautier Izacard, Xavier Martinet, Marie-Anne Lachaux, Timothée Lacroix, Baptiste Rozière, Naman Goyal, Eric Hambro, Faisal Azhar, et al. Llama: Open and efficient foundation language models. *arXiv preprint arXiv:2302.13971*, 2023.
- [Wang *et al.*, 2022a] Zifeng Wang, Zizhao Zhang, Sayna Ebrahimi, Ruoxi Sun, Han Zhang, Chen-Yu Lee, Xiaoqi Ren, Guolong Su, Vincent Perot, Jennifer Dy, et al. Dualprompt: Complementary prompting for rehearsal-free continual learning. In *European Conference on Computer Vision*, pages 631–648. Springer, 2022.
- [Wang *et al.*, 2022b] Zifeng Wang, Zizhao Zhang, Chen-Yu Lee, Han Zhang, Ruoxi Sun, Xiaoqi Ren, Guolong Su, Vincent Perot, Jennifer Dy, and Tomas Pfister. Learning to prompt for continual learning. In *Proceedings of the IEEE/CVF Conference on Computer Vision and Pattern Recognition*, pages 139–149, 2022.
- [Wu *et al.*, 2023] Shengqiong Wu, Hao Fei, Leigang Qu, Wei Ji, and Tat-Seng Chua. Next-gpt: Any-to-any multimodal llm. *arXiv preprint arXiv:2309.05519*, 2023.
- [Young *et al.*, 2014] Peter Young, Alice Lai, Micah Hodosh, and Julia Hockenmaier. From image descriptions to visual denotations: New similarity metrics for semantic inference over event descriptions. *Transactions of the Association for Computational Linguistics*, 2:67–78, 2014.
- [Zhang *et al.*, 2022] Yao Zhang, Haokun Chen, Ahmed Frikha, Yezi Yang, Denis Krompass, Gengyuan Zhang, Jindong Gu, and Volker Tresp. Cl-crossvqa: A continual learning benchmark for cross-domain visual question answering. *arXiv preprint arXiv:2211.10567*, 2022.
- [Zhang *et al.*, 2023] Xi Zhang, Feifei Zhang, and Changsheng Xu. Vqac: A novel visual question answering continual learning setting. In *Proceedings of the IEEE/CVF Conference on Computer Vision and Pattern Recognition*, pages 19102–19112, 2023.
- [Zheng *et al.*, 2023] Zangwei Zheng, Mingyuan Ma, Kai Wang, Ziheng Qin, Xiangyu Yue, and Yang You. Preventing zero-shot transfer degradation in continual learning of vision-language models. *arXiv preprint arXiv:2303.06628*, 2023.
- [Zhu *et al.*, 2023] Hongguang Zhu, Yunchao Wei, Xiaodan Liang, Chunjie Zhang, and Yao Zhao. Ctp: Towards vision-language continual pretraining via compatible momentum contrast and topology preservation. In *Proceedings of the IEEE/CVF International Conference on Computer Vision*, pages 22257–22267, 2023.

A Derivation of Anti-Forgetting for Prompt Tuning

To achieve the goal of anti-forgetting, we expect the model to output the same response given the same image and instruction when soft prompts are updated. Formally, we have

$$f_{LLM}([p_{t+1}^T; e_t^{(img)}; e_t^{(text)}]) = f_{LLM}([p_t^T; e_t^{(img)}; e_t^{(text)}]), \quad (11)$$

where f_{LLM} represents the large language model, and it is frozen during continual learning. $p_{t+1}, p_t \in \mathbb{R}^d$ are the prompts before and after the update of task t . We consider only one prompt for demonstration purposes. $e_t^{(img)} \in$

$\mathbb{R}^{n_i \times d}, e_t^{(text)} \in \mathbb{R}^{n_t \times d}$ represent the n_i, n_t input embedding tokens correspond to the input image and instruction from task t . $[p_{t+1}; e_t^{(img)}; e_t^{(text)}]$ represents that the prompt is concatenated with the input along the sequence dimension. We denote the concatenated input $[p_{t+1}; e_t^{(img)}; e_t^{(text)}]$ and $[p_t; e_t^{(img)}; e_t^{(text)}]$ with a prompt token from task t and task $t+1$ as $Z_{t+1} \in \mathbb{R}^{(1+n_i+n_t) \times d}$ and $Z_t \in \mathbb{R}^{(1+n_i+n_t) \times d}$ respectively.

The input embedding tokens primarily interact with each other in the self-attention layer of LLMs. Therefore, we simplify the objective in Eq. 11 as follows:

$$Attention(Z_{t+1}) = Attention(Z_t) \quad (12)$$

A_{t+1} and A_t are the attention matrix of input Z_{t+1} and Z_t . Then, we expand the attention matrix as follows:

$$Attention(Z_t) = softmax\left(\frac{Z_t W_Q (Z_t W_K)^T}{\sqrt{d_h}}\right) \quad (13)$$

$$= softmax\left(\frac{Z_t W_Q W_K^T Z_t^T}{\sqrt{d_h}}\right) \quad (14)$$

where $W_Q \in \mathbb{R}^{d \times d_h}$ and $W_K \in \mathbb{R}^{d \times d_h}$ are the projection matrix of query and key, $softmax$ represents row-wise softmax function, d_h is the hidden dimension. In Eq.14, W_Q and W_K are unchanged during training since LLMs are frozen. To further simplify the objective, we follow [Boix-Adsera *et al.*, 2023] and assume the query and key matrices W_Q and W_K are diagonal weight matrices and $d_h = d$:

$$W_Q W_K^T = diag(w_Q) diag(w_K)^T, \quad (15)$$

where $w_Q, w_K \in \mathbb{R}^d$ are the diagonal entries of W_Q and W_K . Then, the objective in Eq.12 can be simplified as follows:

$$Z_{t+1} Z_{t+1}^T = Z_t Z_t^T \quad (16)$$

And then, we expand Z_{t+1} and Z_t and Eq.16 can be converted as follows:

$$\begin{bmatrix} p_{t+1}^T \\ e_t^{(img)T} \\ e_t^{(text)T} \end{bmatrix} \begin{bmatrix} p_{t+1} & e_t^{(img)} & e_t^{(text)} \end{bmatrix} = \begin{bmatrix} p_t^T \\ e_t^{(img)T} \\ e_t^{(text)T} \end{bmatrix} \begin{bmatrix} p_t & e_t^{(img)} & e_t^{(text)} \end{bmatrix} \quad (17)$$

$$\begin{bmatrix} p_{t+1}^T p_{t+1} & p_{t+1}^T e_t^{(img)} & p_{t+1}^T e_t^{(text)} \\ e_t^{(img)} p_{t+1} & e_t^{(img)} e_t^{(img)T} & e_t^{(img)} e_t^{(text)T} \\ e_t^{(text)} p_{t+1} & e_t^{(text)} e_t^{(img)T} & e_t^{(text)} e_t^{(text)T} \end{bmatrix} = \begin{bmatrix} p_t^T p_t & p_t^T e_t^{(img)} & p_t^T e_t^{(text)} \\ e_t^{(img)} p_t & e_t^{(img)} e_t^{(img)T} & e_t^{(img)} e_t^{(text)T} \\ e_t^{(text)} p_t & e_t^{(text)} e_t^{(img)T} & e_t^{(text)} e_t^{(text)T} \end{bmatrix} \quad (18)$$

By comparing the two matrix element-wise in Eq.18, we can simplify it as follows:

$$\begin{cases} p_{t+1}^T p_{t+1} = p_t^T p_t \end{cases} \quad (19)$$

$$\begin{cases} e_t^{(img)} p_{t+1} = e_t^{(img)} p_t \end{cases} \quad (20)$$

$$\begin{cases} e_t^{(text)} p_{t+1} = e_t^{(text)} p_t \end{cases} \quad (21)$$

We denote the difference between p_{t+1} and p_t as Δp , i.e., $\Delta p = p_{t+1} - p_t$. Finally, the objective in Eq.11 is summarized as follows:

$$\begin{cases} p_{t+1}^T p_{t+1} = p_t^T p_t \end{cases} \quad (22)$$

$$\begin{cases} e_t^{(img)} \Delta p = O \end{cases} \quad (23)$$

$$\begin{cases} e_t^{(text)} \Delta p = O \end{cases} \quad (24)$$

B Additional Experimental Results

When using InstructBLIP and BLIP2 [Li *et al.*, 2023b] as MLLMs, the task sequence for continual learning is summarized in Table 4 and 5 respectively. We refer readers to InstructBLIP [Dai *et al.*, 2023] for detailed description of datasets. We sample 100 instances for each dataset in task 0 of InstructBLIP to obtain the pre-trained and residual space. For BLIP2, we obtain the pre-trained and residual space on the input embeddings of task 1. The hyper-parameters used for training is summarized in Table 7. For training, we use the same instruction templates in InstructBLIP [Dai *et al.*, 2023]. For inference, we use the instruction templates summarized in Table 6. We only evaluate BLIP2 on the 5 tasks learned during continual learning since BLIP2 has not been instruction-tuned on multiple datasets.

The results on BLIP2 are summarized in Table 8 and Fig.8. Table 8 shows that the previous SOTA method EProj has even worse performance than ER while Fwd-Prompt outperforms ER by 3.20%. It indicates Fwd-Prompt is more robust than ER when training on different MLLMs. Furthermore, Fig.8 shows that Fwd-Prompt has the lowest forgetting and highest forward transfer. Although EProj also alleviates catastrophic forgetting, it leads to negative forward transfer, degrading the performance on GQA from 56.86 to 50.48. In contrast, Fwd-Prompt encourages positive forward transfer and improves the performance on GQA from 56.86 to 58.80.

Table 4: The dataset statistics when continual instruction-tuning InstructBLIP.

Task Order	Dataset	Task Description	# Training Set	# Dev Set	Metric	Source
0	Caption COCO [Chen <i>et al.</i> , 2015]	Image Captioning	567K	5K	CIDEr	Link
	TextCaps [Sidorov <i>et al.</i> , 2020]	Image Captioning with OCR tokens	549K	16K	CIDEr	Link
	VQAv2 [Goyal <i>et al.</i> , 2017]	VQA	443K	214K	ACC	Link
	OKVQA [Marino <i>et al.</i> , 2019]	VQA	9K	5K	ACC	Link
	A-OKVQA [Schwenk <i>et al.</i> , 2022]	VQA	17K	1K	ACC	Link
	OCR-VQA [Mishra <i>et al.</i> , 2019]	VQA	801K	100K	ACC	Link
1	Flickr30k [Young <i>et al.</i> , 2014]	Image Captioning	145K	1K	CIDEr	Link
2	VizWiz [Gurari <i>et al.</i> , 2018]	VQA	20K	4K	ACC	Link
3	TextVQA [Singh <i>et al.</i> , 2019]	VQA with OCR tokens	34K	5K	ACC	Link
4	GQA [Hudson and Manning, 2019]	VQA	94K	13K	ACC	Link

Table 5: The dataset statistics when continual instruction-tuning BLIP2.

Task Order	Dataset	Task Description	# Training Set	# Dev Set	Metric	Source
1	Flickr30k [Young <i>et al.</i> , 2014]	Image Captioning	145K	1K	CIDEr	Link
2	TextCaps [Sidorov <i>et al.</i> , 2020]	Image Captioning with OCR tokens	549K	16K	CIDEr	Link
3	VQAv2 [Goyal <i>et al.</i> , 2017]	VQA	443K	214K	ACC	Link
4	OCR-VQA [Mishra <i>et al.</i> , 2019]	VQA	801K	100K	ACC	Link
5	GQA [Schwenk <i>et al.</i> , 2022]	VQA	94K	13K	ACC	Link

Table 6: The instruction templates for Inference.

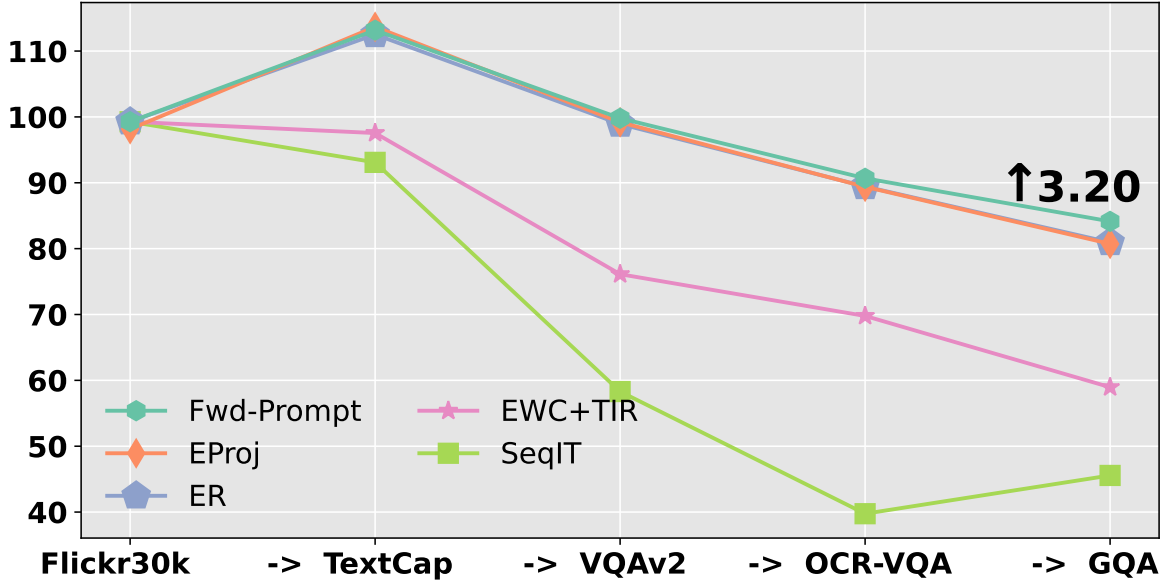
Datasets	Instruction Templates
VQAv2, OKVQA, A-OKVQA, OCR-VQA, VizWiz, GQA Flickr30k, Caption COCO, TextVQA TextCaps	<Image> Question: {} Short answer: <Image> A short image description: <Image> OCR tokens: {}. Question: {} Short answer: <Image> OCR tokens: {}. A short image description:

Table 7: The hyper-parameters used for training Fwd-Prompt.

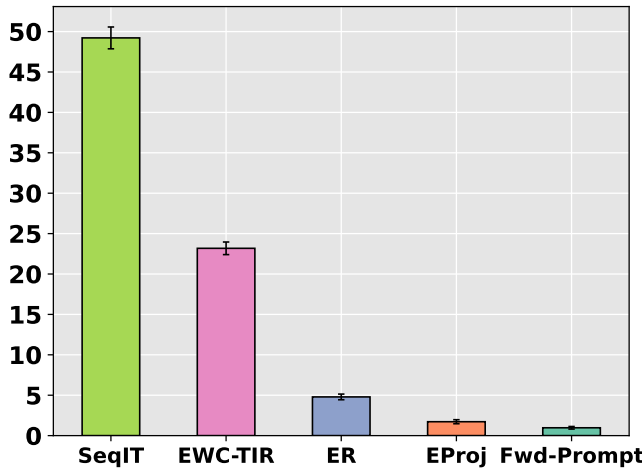
Hyper-Parameters	Value
max epoch	1 for GQA and 5 for others
initial lr	1.00E-05
warmup lr	1.00E-08
warmup steps	1000
weight decay	0.05
batch size	32
num beams	5
output len	VQA-based Tasks: max_len=10, min_len=1
	Image Captioning Tasks: max_len = 80, min_len = 10

Table 8: Comparison with SOTA methods for MCIT. The average accuracy after learning the final task, i.e. \mathcal{A}_5 , is reported. The backbone model is BLIP2. “ER” and “EProj” require storing 1% of old samples for rehearsal.

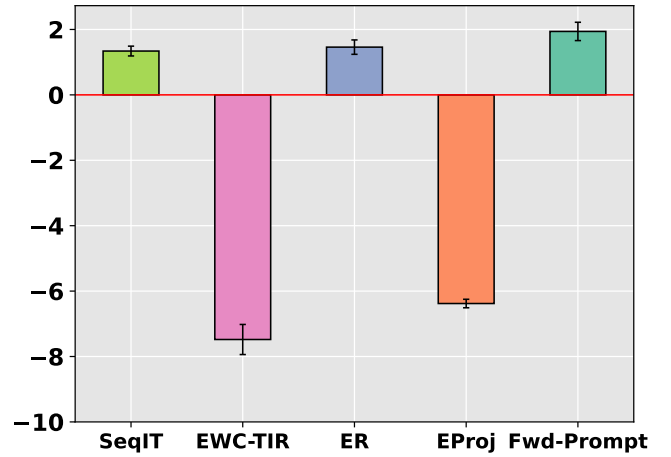
Datasets	Non-CL Baselines		CL Baselines				
	Initial	DirectIT	SeqIT	EWC_TIR	ER	EProj	Fwd-Prompt (Ours)
Flickr30k	80.77	99.27	36.12	66.00	94.35	98.14	<u>98.09</u>
TextCaps	72.04	130.67	26.96	68.35	123.85	<u>126.69</u>	128.65
VQAv2	62.79	73.44	60.75	63.61	65.97	<u>65.98</u>	72.35
OCR-VQA	42.07	63.09	45.80	47.44	62.22	<u>62.37</u>	62.81
GQA	43.80	56.86	58.20	49.38	<u>58.32</u>	50.48	58.80
Average	60.29	84.67	45.57	58.96	80.94	80.73	84.14
Improvement	/	/	0.00	+13.39	+35.37	+35.16	+38.57



(a) Average Accuracy $\mathcal{A}_t \uparrow$



(b) Forgetting $FGT_5 \downarrow$



(c) Forward Transfer $FWD_5 \uparrow$

Figure 8: Comparison with SOTA methods in terms of average accuracy, forgetting and forward transfer. The backbone model is BLIP2.